could not be obtained from an aerial survey. It could determine powdery or jagged rock out-croppings and the size and distinguishing features of the craters.

The team of astronauts and teleoperators working on the moon would examine candidate sites in detail to determine susceptibility to moonquakes, the depth and bearing strength of granular material, and the presence and strength of large rock formations.

The preparation of the selected site for the facility would take many months, much longer than astronauts could stay on the moon. The site preparation would be accomplished by robots and Earth-controlled teleoperators. Robots would grade the soil compaction and do the trenching. Earth-controlled teleoperators would assemble and maintain the robotic construction equipment and control the over-all operation. The permanent control center and a habitat for astronauts would be built. It is expected that astronauts would return to the moon for this phase of construction, which would be a complicated installation requiring the intelligence and adaptability of men. The astronauts would use teleoperators to transfer prefabricated sections of the control center and habitat from the lunar shuttles to the previously prepared foundations. Astronauts and teleoperators would then work together carefully assembling and testing the control center and habitat.

Astronauts would later return to the moon to perform the checkout and activation operations, using teleoperators where required. Astronauts would provide the on-site expertise and judgement needed for activating the facility. Although the robots intended to operate the facility would have been proven and "trained" in a simulation facility on the Earth, the astronauts would work closely with the operating robots during the initial operations to ensure that the robots are able to operate the Earth observation facility for an extended period of time.

Astronauts would not be needed to operate the facility on a routine basis, since the robots would maintain the facility, receive and warehouse supplies and spare parts, and ship scientific data and records back to Earth. During these extended unmanned operating periods, Earth-controlled teleoperators would be used to maintain and repair the robots to adjust, align, calibrate, and repair experiments and facility equipment. Astronauts would return to the facility only when on-site operations are required to refurbish it or to install and check out new experiments, sensors, or computing systems.

The creation of astronaut-teleoperator-robot teams will provide a practical technique for constructing large space facilities, and operating the facilities over several decades. Similar approaches can eventually be used for exploring and developing the planets. The robots can rove and do simple tasks. The teleoperators can extend man's sophisticated capabilities across great distances. Man can use his experience, judgement, and associative thinking abilities to construct and operate large and complex facilities in space. The integration of man, teleoperators, and robots will create flexible teams with composite abilities far superior to those of the individual components.

References

[1] Johnsen, E. G. and Corliss, W. R., "Recent History," *Human Applications in Teleoperator Design and Operation*, Wiley, New York, 1971, pp. 6–8.

[2] Atomic Energy Commission, *Proceedings of the 1964 Seminars on Remotely Operated Special Equipment*, Vol. 1, AEC CONF-640508 and AEC CONF-641120, *1964*.

[3] Clark, J. W., The Mobot Mark II Remote Handling System, *Proceedings of the Ninth Hot Laboratory and Equipment Conference*, American Nuclear Society, Chicago, Ill., 1961, pp. 111–120.

[4] Karinen, R. S. et al., *Summary Report Mobile Remote Handler*, Rep. SCDC-878, 1957, Sandia Corp.

[5] Nickel, V. L., "Investigation of Externally Powered Orthotic Devices," Final Project Rept., 1964, Rancho Los Amigos Hospital, Downey, Calif.

Air Film Cooling in a Nonadiabatic Wall Conical Nozzle

DONALD R. BOLDMAN,* STEVE S. PAPELL,† and ROBERT C. EHLERS‡
NASA Lewis Research Center, Cleveland, Ohio

Nomenclature

c_p = specific heat
h = heat-transfer coefficient
K = constant in Eq. (3)
m = mass flow rate
P = pressure
R = nozzle radius
S = slot height
T = temperature
u = velocity
x = distance along wall from coolant slot
z = axial distance from coolant slot
α = thermal diffusivity
η = adiabatic wall film cooling effectiveness
η' = nonadiabatic wall film cooling effectiveness
$\phi, \phi_1, \phi_2, \phi_3$ = exponents defined by Eqs. (3–6)

Subscripts

c = coolant condition at slot
L = based on local conditions
w = wall condition
0 = stagnation condition
∞ = freestream condition

Superscripts

* = geometric throat
o = condition with no film cooling

Introduction

FILM cooling techniques provide a means of preventing structural deterioration of components such as turbine blades and rocket nozzles which experience very high local heat fluxes. Two procedures have been followed in predicting the effects of film cooling on heat transfer; namely, correlation methods[1–3] and various boundary-layer theories.[4,5] Boundary-layer methods will undoubtedly receive increased emphasis, particularly when the coolant flow rate is critical to performance; however, in many applications it is acceptable to apply the simpler correlation methods.

Using the apparatus of Ref. 6, the present study evaluates various forms of a correlation method as applied to an air film-cooled conical nozzle operating with a heated-air main stream and a water-cooled wall.

Several film cooling studies in the literature have dealt with nonaccelerated flow over adiabatic walls. In many of these studies, correlations of the Hatch-Papell[1] type were applied with reasonable success. It has also been shown that a satisfactory correlation of film cooling data in the highly accelerated flow of an adiabatic-wall rocket nozzle could be obtained with a slight modification of the method of Ref. 1.[2] Lieu[3] modified the film cooling effectiveness η in order to

Received December 29, 1971; revision received February 22, 1972.
Index categories: Nuclear Propulsion; Liquid Rocket Engines; Jets, Wakes, and Viscid–Inviscid Flow Interactions.

* Aerospace Engineer. Member AIAA.
† Aerospace Engineer.
‡ Aerospace Engineer.

extend the method to configurations with externally cooled walls. The results of the present study are premised on the combined findings of Refs. 2 and 3 with the latter work providing a basis for comparison of the present data.

Apparatus

The apparatus consisted of a 16.5 cm (6.5 in.) inside diameter by 43.2 cm (17.0 in.) long adiabatic pipe inlet coupled to a 30° half angle of convergence by 15° half angle of divergence water-cooled conical nozzle as shown in Fig. 1. An annulus having a height of 0.056 cm (0.022 in.) provided tangential injection of the film coolant. Air was used for the main stream fluid and the film coolant. All tests were conducted at a film-coolant temperature of 314°K (566° R), main stream stagnation temperature of 539° K (970° R), and stagnation pressure of 207 N/cm² (300 psia). Nozzle heat-transfer rates and wall temperatures were obtained with plug type heat flux meters.[6] Film coolant flow rates of nominally 1, 2, 5, and 10% of the main flow were used in the tests.

Results

The general form of the correlation for tangential injection is

$$\eta = e^{-\phi} \tag{1}$$

where η is the film cooling effectiveness and ϕ is a function of the geometry, heat transfer coefficient, coolant properties, and the main to coolant-flow velocity ratio. As suggested in Ref. 3, the film cooling effectiveness should be modified for nonadiabatic walls in order to provide a measure of the difference in wall temperature due to film cooling relative to the difference between the wall temperature in the absence of film cooling and the coolant temperature. Accordingly, η will be redefined as η' where

$$\eta' = (T_w{}^0 - T_w)/(T_w{}^0 - T_c) \tag{2}$$

The general expression for ϕ is

$$\phi = \left[\frac{2\pi h^0 Rx}{(mc_p)_c} - K\right]\left(\frac{Su_\infty{}^0}{\alpha_c}\right)^{0.125} f\left(\frac{u_\infty{}^0}{u_c}\right) \tag{3}$$

where $f = 1.0 + 0.4\tan^{-1}[(u_\infty{}^0/u_c) - 1.0]$ when $u_\infty{}^0/u_c \geq 1.0$

and $f = (u_c/u_\infty{}^0)^{1.5[(u_c/u_\infty{}^0)-1.0]}$ when $u_\infty{}^0/u_c \leq 1.0$

The value of ϕ in the preceding correlation will be evaluated in three different ways using the experimental results of the present study as input. The expressions for ϕ are as follows:

$$\phi_1 = \{[2\pi h^0 R/(mc_p)_c](Su_\infty{}^0/\alpha_c)^{0.125} f(u_\infty{}^0/u_c)\}_{x=0}\, x \tag{4}$$

$$\phi_2 = \{[2\pi h^0 Rx/(mc_p)_c](Su_\infty{}^0/\alpha_c)^{0.125} f(u_\infty{}^0/u_c)\}_L \tag{5}$$

$$\phi_3 = \left\{\left[2\pi \int_0^x h^0 R\, dx/(mc_p)_c\right](Su_\infty{}^0/\alpha_c)^{0.125} f(u_\infty{}^0/u_c)\right\}_L \tag{6}$$

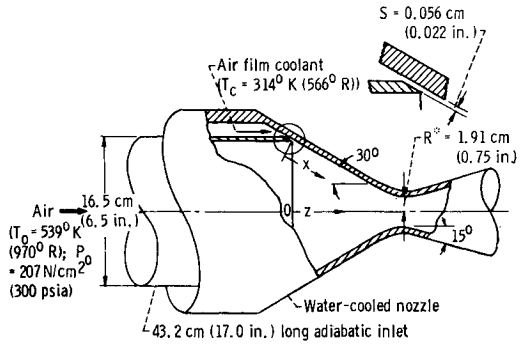

Fig. 1 Nozzle configuration.

Equation 4 represents the method of Ref. 3 except for the value of K which was assumed to be zero.[2] Note that ϕ_1 is dependent only on the slot conditions and distance x. The expression for ϕ_2 has the same form as Eq. 4; however h^0, R, and $u_\infty{}^0$ are local rather than slot values. In Eq. 6, the integrated average of the product of the local heat-transfer coefficient h^0 and radius R is used as suggested in Ref. 2, rather than the local values.

The results of the three forms of the correlation are presented in Fig. 2§ in terms of the predicted wall temperature distributions for the four coolant flow rates. Differences in the predicted temperature distributions arising from the use of ϕ_2 and ϕ_3 are negligible for all of the coolant flow rates. The differences in the predicted temperature distributions, apparent when ϕ_1 is used rather than ϕ_2 or ϕ_3, do not become appreciable until $m_c/m_\infty{}^0 = 0.10$ (Fig. 2d). At a velocity ratio of about 1.0 the use of ϕ_2 or ϕ_3 yields an improvement over predictions based on ϕ_1, particularly in the vicinity of the coolant injection (Fig. 2b). The agreement at these conditions is quite good—within about 5% of the experimental distribution.

Comparison of the experimental wall temperature distributions in Fig. 2 with the results for $m_c = 0$ indicates that the effects of film cooling were evident at least as far downstream as the throat. Also, it can be noted that the distribution at the high coolant flow rate ($m_c/m_\infty{}^0 = 0.10$) is not smooth. Hot spots in which the local wall temperature nearly approached the value for $m_c = 0$ are indicated at $z = 6.6$ cm (2.6 in.)

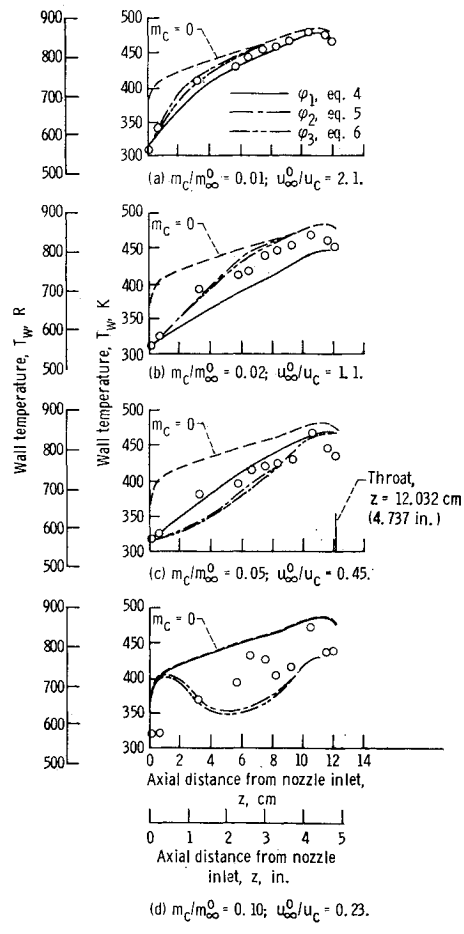

Fig. 2 Measured and predicted wall temperature distributions. $T_0 = 539°$ K(970° R); $P_0 = 207$ N/cm² (300 psia).

§ In Fig. 2; (a) $m_c/m_\infty{}^0 = 0.01$, $u_\infty{}^0/u_c = 2.1$; (b) $m_c/m_\infty{}^0 = 0.02$, $u_\infty{}^0/u_c = 1.1$; (c) $m_c/m_\infty{}^0 = 0.05$, $u_\infty{}^0/u_c = 0.45$; (d) $m_c/m_\infty{}^0 = 0.10$, $u_\infty{}^0/u_c = 0.23$.

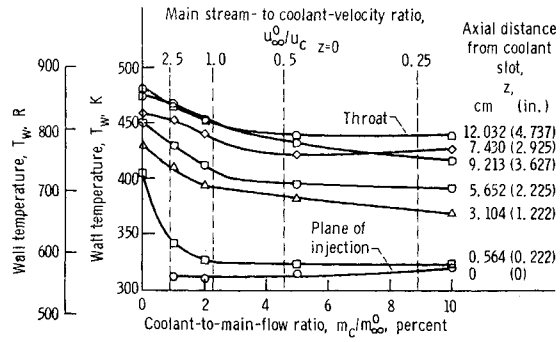

Fig. 3 Variation of wall temperature with coolant flow rate, $T_0 = 539°$ K (970° R); $P_0 = 207$ N/cm² (300 psia); $m_\infty{}^0 = 4.1$ kg/sec (9.0 lb/sec); $u_\infty{}^0 = 11.0$ m/sec (36.1 ft/sec).

and at $z = 10.4$ cm (4.1 in.). These hot spots are possibly the result of extreme mixing caused by the low main stream velocity relative to the coolant injection velocity ($u_\infty{}^0/u_c = 0.23$) or flow separation. Similar hot spots were noted when the pipe inlet was rotated 180° relative to the nozzle indicating that nonuniformities in the flow pattern at the slot were probably not responsible for this behavior.

The decrease in wall temperature with increasing coolant flow rate appears to reach an optimum as shown in Fig. 3. At nearly all of the stations, a large reduction in wall temperature occurs in the coolant flow range of $0 < m_c/m_\infty{}^0 < 0.02$. At higher values of $m_c/m_\infty{}^0$, the reduction in wall temperature is small and in some cases, the wall temperature actually increases (hot spots at $m_c/m_\infty{}^0 = 0.10$). The velocity ratio $u_\infty{}^0/u_c$ corresponding to the optimum reduction in wall temperature is approximately 1.0; that is, the optimum injection velocity appears to be equal to or possibly slightly greater than the main stream velocity.

Summary

The results of the present experimental study in a cooled 30° half angle of convergence nozzle tend to be consistent with the results of Ref. 3 which indicated 1) the feasibility of using a modified effectiveness η' to correlate film cooling in nonadiabatic wall accelerated flows provided the main stream to coolant velocity ratio at the slot is about 1.0, and 2) that a main stream to coolant velocity ratio of about 1.0 provides the optimum cooling effectiveness. A slight improvement in the correlation of Ref. 3 was obtained by using local rather than slot conditions in the evaluation of ϕ. It should be recognized that the results of this study were based on a single set of main stream flow conditions and geometric parameters. Therefore, extrapolation to other conditions must await further verification.

References

[1] Hatch, J. E. and Papell, S. S., "Use of a Theoretical Flow Model to Correlate Data for Film Cooling or Heating an Adiabatic Wall by Tangential Injection of Gases of Different Fluid Properties," TN D-130, 1959, NASA.

[2] Lucas, J. G. and Golladay, R. L., "Gaseous-Film Cooling of a Rocket Motor with Injection Near the Throat," TN D-3836, 1967, NASA.

[3] Lieu, B. H., "Air-Film Cooling of a Supersonic Nozzle," NOLTR 64-65, Aug. 1964, Naval Ordnance Lab., White Oak, Md.

[4] Seban, R. A. and Back, L. H., "Effectiveness and Heat Transfer for a Turbulent Boundary Layer with Tangential Injection and Variable Free-Stream Velocity," *Journal of Heat Transfer*, Vol. 84, No. 3, Aug. 1962, pp. 235–244.

[5] Beckwith, I. E. and Bushnell, D. M., "Calculation by a Finite-Difference Method of Supersonic Turbulent Boundary Layers with Tangential Slot Injection," TN D-6221, 1971, NASA.

[6] Boldman, D. R., Neumann, H. E., and Schmidt, J. F., "Heat Transfer in 30° and 60° Half-Angle of Convergence Nozzles with Various Diameter Uncooled Pipe Inlets," TN D-4177, NASA.

Parameters Influencing Dynamic Stability Characteristics of Viking-Type Entry Configurations at Mach 1.76

CHARLES H. WHITLOCK* AND PAUL M. SIEMERS III†
NASA Langley Research Center, Hampton, Va.

Nomenclature‡

C_m	= pitching moment coefficient
C_{mq}, $C_{m\dot{\alpha}}$	= $\partial C_m/\partial(qD/2V)$, $\partial C_m/\partial(\dot{\alpha}D/2V)$, (rad^{-1})
d_s, D	= sting diameter, model diameter, m
l_s	= sting length, m
R_N	= Reynolds number
V	= freestream velocity, m/sec
α	= angle of attack, deg
θ	= balance oscillation amplitude, deg
ω	= body oscillation frequency, rad/sec

Introduction

BLUNT conical configurations have been considered for entry vehicles because of their high-drag characteristics. Early tests[1] discovered that such configurations may be dynamically unstable in the transonic speed range; however, results were inconsistent. Other tests[2,3] defined angle of attack as one parameter which might explain the inconsistencies, and forced-oscillation tests[4,5] were conducted to define the extent of nonlinearity with angle of attack.

Additional inconsistencies were uncovered by the forced oscillation data. A number of parameters may contribute to the inconsistencies. The effects of Reynolds number, reduced frequency parameter, and tunnel vibration were not understood, and data at low angles of attack were inconsistent for similar configurations when model size was changed. Attempts to simulate the motions of a full-scale flight vehicle with the tunnel data were unsuccessful. Applicability of data from in-plane forced-oscillation techniques to predict flight motions which cross the angle-of-attack plane (elliptic or conical motions) was questioned. It was also realized that the forced-oscillation data were average (or effective) values over a small amplitude range about a nominal angle of attack but motion studies require values based on the instantaneous angle of attack. The effect of changes in base geometry was also a question. Some results[4,5] indicated minimum effects although other data[6] showed that the transonic instability could be completely eliminated by proper selection of base geometry.

A two-part investigation was initiated to define the important variables which influence the transonic dynamic stability characteristics of blunt-conical configurations. Free-oscillation tests of three Viking-type configurations were conducted in Tunnel A of the von Kármán Gas Dynamics Facility at the Arnold Engineering Development Center. A parallel effort developed a technique for correcting either forced- or free-oscillation damping data to values based on the instantaneous angle of attack. This note will briefly summarize the results of these investigations using Mach 1.76 results.

Wind-Tunnel Results

The configurations tested in the Tunnel A facility are shown in Fig. 1. Model 721 is an early proposed design from which the present VIKING configuration was derived. It is the only configuration of this series which had been subject to previous

Received January 17, 1972; revision received March 20, 1972.
Index categories: Spacecraft Attitudes Dynamics and Control; Entry Vehicle Dynamics and Control; Nonsteady Aerodynamics.

* Aerospace Engineer. Member AIAA.

† Aerospace Engineer.

‡ Dots over symbols indicate derivatives with respect to time.